

LES AND DES SIMULATIONS OF PARTICLE PATHS INSIDE A SMALL SAMPLING CYCLONE SEPARATOR

Ricardo de Vasconcelos Salvo, rvsalvo@hotmail.com

Francisco José de Souza, fjsouza@mecanica.ufu.br

Diego Alves de Moro Martins, moromartins@gmail.com

Faculdade de Engenharia Mecânica – FEMEC, Universidade Federal de Uberlândia – UFU, Av. João Naves de Ávila, 2121, Santa Mônica, Uberlândia, Brazil

Abstract. *This paper presents the simulation of a small sampling cyclone separator, aiming at the investigation of the influence of turbulent dispersion, turbulence modeling (where two different LES models and a DES model were used) on the cyclone grade efficiency. The particles are homogeneously distributed through the inlet area and are injected at the same velocity as the fluid. The computations are performed assuming one-way coupling. The fluid phase is treated as a continuum (in an Eulerian framework) and the particles are treated as a discrete phase (in a Lagrangian framework). The numerical tool utilized is an in-house code based on the finite volume method in three-dimensional unstructured grids with the SIMPLE algorithm for pressure-velocity coupling. The results are physically consistent and show some interesting features about the influence of boundary conditions for particle phase and the influence of turbulence modeling in the grade efficiency and particles paths inside the cyclone.*

Keywords: *Cyclone Separator, DES, LES, Eulerian-Lagrangian, Grade efficiency*

1. INTRODUCTION

Reverse flow cyclones are probably the most widely used separator devices in industrial environments, being applied in many industrial branches (ranging from food and pharmaceutical industries to mining and petrochemical industries). Their popularity is based on their relative geometrical simplicity, low manufacturing, operational and maintenance costs. Although these devices are structurally simple, normally being a cylinder-on-cone structure with a tangential (or scroll) type inlet and two outlets (one for the gas at the top, and other for the solids at bottom), their design is complicated and hardly optimized, once the flow field within these devices is extremely complex (Hoffman and Stein, 2008). Due to this complexity CFD simulations became, in the last few years, one important tool in cyclone design allowing a detailed analysis of the flow field in the interior of these devices.

Although CFD simulations do offer good predictions of the flow field in the interior of cyclone separators this is not a closed subject, since the Reynolds number in these equipment is normally high (over 200,000) and consequently direct numerical simulations (where all the scales are resolved) cannot be applied, requiring the usage of turbulence models. It is known from literature that traditional RANS turbulence models do not work properly in strong rotating flows, and even the more complex RSM turbulence model normally has to be run unsteady (Slack et al. (2000); Wegner et al. (2004); Bernardo (2005); Narasimha et al. (2006); Narashimha et al. (2007); Shalaby (2007), to name a few). Recently several authors decided to use LES models for the simulation of these devices, knowing that although much more expensive it theoretically can supply more information about the flow field, especially about the instantaneous velocity and pressure fields and consequently provide additional information about secondary flows and other phenomena, like the precessing vortex core (Slack et al. (2000); Hoekstra et al. (2000); Derksen (2003); Derksen et al. (2006); Narasimha et al. (2006); Narasimha et al. (2007); Gronald and Derksen. (2010); Pisarev et al. (2010); among others).

Another issue that has to be considered is the modeling of the dispersed phase. Basically two different approaches are currently being applied to the simulation of cyclone separators for the prediction of the dispersed phase motion: two fluid models (in an Eulerian-Eulerian framework) and dispersed phase models based in an Eulerian-Lagrangian framework. Two fluid models are not restricted to small particle volume fraction and basically have a fixed cost, which, according to Garcia et al (2007) is about 80% for each new phase, meanwhile the computational cost of the Eulerian-Lagrangian model is directed linked to the number of particles being simulated, and the maximum number of particles will be limited by computational time and RAM memory available. An other important aspect of this methodology that requires special attention is the coupling between phases. Elghobashi (1991, apud Peltola, 2009) presents a diagram, Fig. 1, in which he classifies the coupling between the particles and the turbulence of the surrounding flow into three different categories based on the particles volume fraction or on the distance between them.

According to Elghobashi's diagram, flows with particle volume fraction bigger than $1.0E-6$ should be tackled as two-way simulations, and flows with particle volume fraction bigger than $1.0E-3$ should be treated as four way simulations. In the specific case of cyclone simulations, it important to consider the strong centrifugal force field and bear in mind that it causes the particles to concentrate at the cyclone wall, as shown in an interesting work by Shaohua et al. (2009). The author showed that the volumetric solid concentration in his experimental cyclone separator varied from less than 0.01 in the central region to more than 0.26 in the near the wall. Obviously, this data is dependent on the

cyclone geometry and operational parameters (including particles diameter and density), but this behavior is expected for all cyclone separators, as for example in the work of G. Wan et al., (2008), in which they found that particle concentration in the near wall region was almost 200 times the concentration in the cyclone center for their simulated cyclone. Thus, even if a cyclone is operating with a low solids volumetric fraction, a two-way simulation may be needed, at least in the near wall region. Although from a theoretical point of view this is true, from a more practical view most of the cyclone simulations are done considering only one-way coupling and good results, at least in the acquisition of engineering parameters like pressure drop, particle cut-size and collection efficiency, are being obtained.

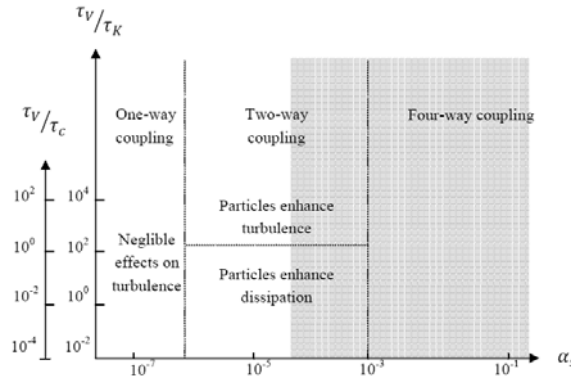


Figure 1. Elghobashi's (1991, apud Peltola 2009) diagram for the classification of particle-turbulence coupling.

In the present work, the two-phase flow in a small sampling cyclone operating with a moderate Reynolds number (22,000) was simulated. The numerical code used is an in-house code based on the finite volume method in three-dimensional unstructured grids with the SIMPLE algorithm for pressure-velocity coupling. The dispersed phase is simulated in a Lagrangian framework, considering a one-way coupling between fluid and particles. The results for grade efficiency were compared with experimental data and are physically consistent, though overpredicted for all particle diameters. The effects of turbulence dispersion and turbulence models on the grade efficiency are investigated, and some insight in particles behavior inside the cyclone separator is provided.

2. MATHEMATICAL FORMULATION

2.1. The gas phase

The conservation of mass and the Navier-Stokes equations for a general incompressible linear (Newtonian) viscous flow can be written, adopting the Einstein convention, respectively as:

$$\frac{\partial \rho u_i}{\partial x_i} = 0 \quad (1)$$

$$\frac{\partial \rho u_i}{\partial t} + \frac{\partial}{\partial x_j} (\rho u_i u_j) = -\frac{\partial p}{\partial x_i} + \frac{\partial}{\partial x_j} \left[\nu \left(\frac{\partial u_i}{\partial x_j} + \frac{\partial u_j}{\partial x_i} \right) \right] \quad (2)$$

By applying a filtering process to the above equations it is possible to separate the larger scales, which are related to the lowest frequencies, from the smallest scales, which are related to the higher frequencies. Equation (2) may be rewritten as:

$$\frac{\partial \rho \bar{u}_i}{\partial t} + \frac{\partial}{\partial x_j} (\rho \bar{u}_i \bar{u}_j) = -\frac{\partial \bar{p}^*}{\partial x_i} + \frac{\partial}{\partial x_j} \left[(\nu + \nu_t) \left(\frac{\partial \bar{u}_i}{\partial x_j} + \frac{\partial \bar{u}_j}{\partial x_i} \right) \right] \quad (3)$$

In Eq. (3), the over-bar denotes a filtered quantity, the asterisk denotes the modified pressure and ν_t is the turbulent viscosity (this term represents the energy dissipation present on the smallest scales of flow, which are not resolved in LES, so it has to be modeled).

2.2. The dispersed phase

The dispersed phase is treated in a Lagrangian framework. The equation of motion for each particle follows Newton's second law.

$$\frac{du_p}{dt} = F_D(u - u_p) + a \quad (4)$$

In Eq. (4) the first term on the right hand side is the drag force experienced by the particle, F_D is given by Eq. (5) and “a” is the acceleration term, which in the present work considers only the gravitational and buoyancy forces Eq. (6):

$$F_D = \frac{18\mu}{\rho_p d_p^2} \frac{C_D Re_p}{24} \quad (5)$$

$$a = \frac{g(\rho_p - \rho)}{\rho_p} \quad (6)$$

In Eq. (5), Re_p and C_D are the particle Reynolds number, Eq. (7), and the drag coefficient, respectively:

$$Re_p \stackrel{\text{def}}{=} \frac{\rho d_p |u_p - u|}{\mu} \quad (7)$$

3. TURBULENCE MODELS

It is known from the literature (Hoffman and Stein, 2008; Derksen, 2003) that turbulence plays a crucial role in particle behavior inside cyclone separators, and may considerably affect the separation efficiency. Thus, the correct turbulence modeling is of fundamental importance in the simulation of such devices. Considering this, three different turbulence models were used in this work, namely, the dynamic and Yakhot LES models, and the SST-DES model of Strelets. More information on these models can be found, respectively, in: Lilly. (1992); Yakhot et al. (1986); Strelets (2001).

4. NUMERICAL METHOD

4.1. Numerical code

For the simulations, the computational code UNSCYFL3D (Unsteady Cyclone Flow – 3D), was used. This in-house code is being developed as a dedicated tool for simulating highly rotational flows, aiming at cyclones/hydrocyclones separators and swirl tubes. It is based on the finite volume method in unstructured grids, which enables the faithful representation of complex geometries. The SIMPLE (Semi-Implicit Method for Pressure-Linked Equations) algorithm is used for the velocity-pressure coupling. In all the simulations accomplished in this work the time-advancement was second-order and the central differencing scheme was employed for the advective and diffusive terms of the momentum equations. The non-smoothness of the grid and non-orthogonality effects are also taken into account (Ferziger and Peric, 2002). For the solution of the linear systems the biconjugate gradient (Ferziger and Peric, 2002) and the algebraic multigrid (Notay, 2008) methods are used.

For the dispersed phase, each particle is tracked in a Lagrangian framework by the particle-localization algorithm proposed by Haselbacher et al. (2007). The particle equations of motion were combined with the particle trajectory equation, Eq. (15), and analytically integrated, assuming that drag force, fluid velocity and acceleration are constant. While this might sound as a brutal simplification, it is a reasonable approximation if the time step is small, which is typically used in LES.

$$\frac{dx_p}{dt} = u_p \quad (15)$$

The resulting equations, Eq. (16) and Eq. (17) were implemented.

$$u_p^{n+1} = u^n + e^{-\Delta t/\tau_p}(u_p^n - u^n) - a\tau_p(e^{-\Delta t/\tau_p} - 1) \quad (16)$$

$$x_p^{n+1} = x^n + \Delta t(u^n + a\tau_p) + \tau_p(1 - e^{-\Delta t/\tau_p})(u_p^n - u^n - a\tau_p) \quad (17)$$

In the above equations, x_p is the particle position vector; “a” is the acceleration term, given by Eq. (6); τ_p is given by $1/F_D$, where F_D is the drag force defined in Eq. (5); the subscript “p” denotes particle, the superscript “n+1” denotes the calculated variable at the new time step and the superscript “n” denotes the calculated variable at the previous time step.

Currently two drag models are implemented for spherical particles; the Morsi and Alexander (1972) drag model and the one proposed by Schiller and Naumann (1935). The last one was used in the simulations shown here.

4.2. Numerical procedure

The cyclone geometry simulated is a small sampling cyclone, as can be seen in Fig. 2. This is the same geometry experimentally studied by R. Xiang et al. (2001) and numerically simulated by Chuah et al. (2006). The fluid is treated as air with constant density 1.205 Kg/m^3 and viscosity $1.82\text{E-}05 \text{ Kg/m.s}$. Initially, a steady case was solved with the SST turbulence model, using a first order upwind scheme for the conservation equations and convergence criteria of $1.0\text{E-}05$. Then the resulting flow field was used as an initial field for the transient simulations. All the transient simulations were performed with the CDS scheme for conservation equations and a convergence criterion of $1.0\text{E-}04$, with a time step of $1.0\text{E-}05 \text{ s}$.

The average residence time for this cyclone is approximately 0.1 s. In order to guarantee that a statistically established regime had been reached, 0.5 s of physical time were simulated. Then the last instantaneous field was used as an initial field for the gas-solid simulations. As for the solid phase, monodisperse polystyrene latex (PSL) particles with density 1050 kg/m^3 and diameters 0.5, 1.0, 1.5, 2.0, 2.5, 3.0, 3.5, 4.0, 4.5, 5.0, 5.5, 6.0 μm , were simulated.

The main cyclone dimensions are shown in Tab. 1.

Table 1. Geometrical dimensions of the simulated cyclone

Dimension	Length (m)	Dimension ratio (dimension/ D_c)
Body diameter, D_c	0.031	1
Gas outlet diameter, D_e	0.0155	0.5
Inlet height, a	0.0125	0.4
Inlet Width, b	0.005	0.16
Cyclone height, H	0.077	2.5
Cylinder height, h	0.031	1
Gas outlet duct length, S	0.0155	0.5
Cone bottom opening, B	0.0194	0.625

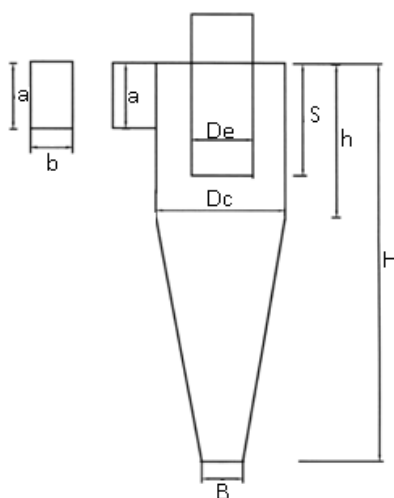


Figure 2. Schematic diagram of the simulated cyclone, adapted from R. Xiang et al. (2001)

In this work, the wall thickness of the vortex finder was assumed to be $D/12.4$, since no reference was found for it.

4.3. Boundary conditions

Boundary conditions for the gas phase:

- At the inlet a normal, uniform velocity profile of 10.667 m/s, yielding a Reynolds number of approximately 22,000, was used;
- At the overflow outlet the pressure was prescribed;
- All the cyclone walls were considered as no-slip.

Boundary conditions for the solid phase:

- The particles were injected with the same velocity as the fluid at the inlet faces (one particle of each diameter in each inlet face center). As the simulations were performed with one-way coupling, the injection

was not made continuously (only a particle pulse was utilized for each simulation). The total number of particles injected into the cyclone was 3,036 in each one of the simulations;

- At the wall particles were reflected considering a perfectly elastic collision;
- For determining the grade efficiency two different boundary conditions were tested:
 - In the first, particles were allowed to exit the cyclone through the bottom wall (particles that touched the cone apex wall were considered as collected) and through the overflow, particles that crossed the outlet faces were considered as lost (escaped) – In this work this condition will be denoted as “Collected&Trapped”;
 - In the second, the particles that crossed the outlet faces were considered as lost, but particles were not able to pass through the cone apex (they were reflected, just like any other particle-wall collision) – In this work this condition will be denoted as “Escaped”.

4.4. Numerical grid

A mesh with approximately 380,000 hexahedral elements was used. This mesh was generated with the mesh generator ICEM-CFD, and can be seen in Fig. 3.

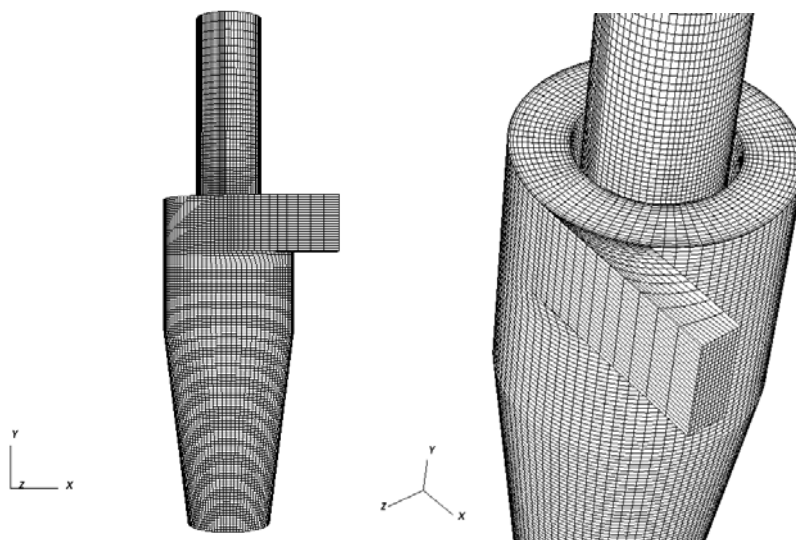


Figure 3. Hexahedral mesh with approximately 380,000 elements used in all the simulations.

5. RESULTS

5.1. Turbulent dispersion analysis

In order to analyze the effects of turbulent dispersion on the particle, five simulations were run. In all these simulations the Yakhot turbulence model was used, and a total time of 1.0 s, after the particle injection, was simulated. The only difference among these simulations is the injection timing, as described in Tab 2.

Table 2. Description of the five cases used in the study of turbulent dispersion.

Case	Initial Time (s)	Time when particles were injected (s)	Total simulated time (s)	Turbulence model
- a -	0.5	0.5	1.5	Yakhot
- b -	0.5	0.525	1.525	Yakhot
- c -	0.5	0.55	1.55	Yakhot
- d -	0.5	0.575	1.575	Yakhot
- e -	0.5	0.6	1.6	Yakhot

The grade efficiency was calculated for all the cases described above and the results show that, although turbulent dispersion is important in the separation of the dispersed phase, simply changing the injection timing does not seem to affect the grade efficiency, as can be seen in Fig. 4. In these simulations the particles were only allowed to leave the cyclone through the overflow (“Escaped” condition).

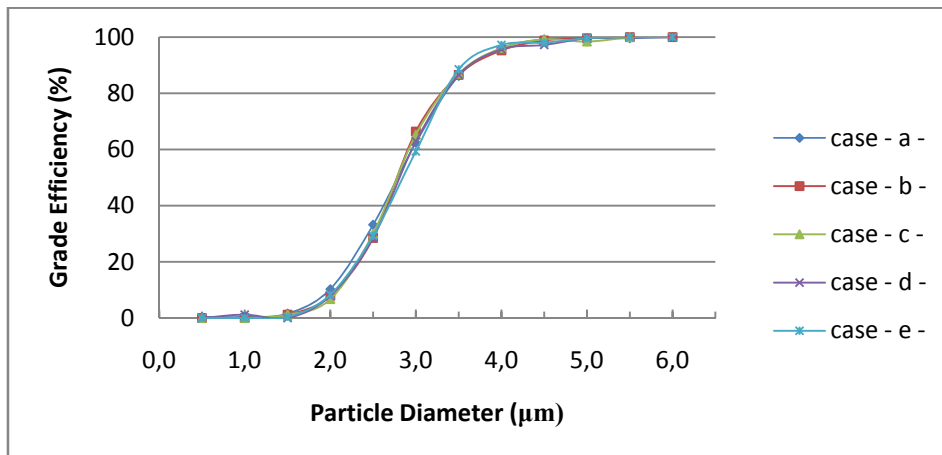


Figure 4. Effect of turbulent dispersion on the collection efficiency, for the cases described in Tab. 2.

5.2. Influence of the boundary conditions of the solid phase in the separation efficiency

In order to calculate the grade efficiency, simulations were performed with two different collection criteria for the particulate phase. In the first, the grade efficiency was defined as the difference between particles that were injected and particles that escaped through the overflow divided by the number of particles injected. This mimics the criterion used in the experimental work of R. Xiang. However, the particle-wall collisions are treated as being perfectly elastic (no energy loss due to the collision), thus the particles that have not escaped through the overflow keep flowing within the cyclone cone.

The combination of these conditions (perfectly elastic collisions and particles escaping through the overflow) with the unsteady cyclone flow field, which presents strong turbulence fluctuations and low frequency periodical movements like the PVC (precessing vortex core), leads to an unrealistic condition: if the simulation continues infinitely the only particles remaining in the cyclone would be those with 100 % grade efficiency. Conversely, the grade efficiency curve would present only either zero or 100 % efficiency if the sampling time tends to infinity. Fig. 5 shows this trend. Because the flow is turbulent and periodic, it might be speculated that, if one particle of a certain diameter was carried at some moment by an upward flow and escaped though the overflow, so will eventually all the others of that diameter. According to Derksen et al. (2006), it is most likely that the PVC does not affect the separation process; the relaxation times of most particles are much smaller than the period of a precession cycle. Nevertheless, by considering a closed underflow with perfectly elastic collisions, it is possible that particles start to suffer some PVC effects through the flow field, and this might affect separation.

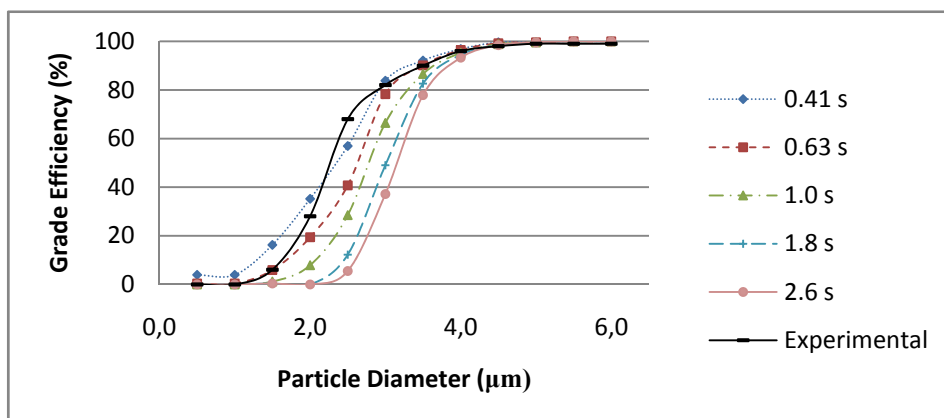


Figure 5. Evolution of the grade efficiency with simulation physical time – criterion base on particles escaping though the overflow.

Derksen (2003) states that the convergence of the flow statistics is typically reached after $25 D/U_{in}$, but, when considering the particulate phase he found that some particles took a little longer than $200 D/U_{in}$ to be exhausted or separated. Although a direct comparison cannot be made, as this is a completely different cyclone, this can be used as a raw estimate of the required time for all the injected particles to leave the cyclone. The physical time corresponding to

200 D/U_{in} in the present simulations would be 0.58 s, showing some agreement with the 0.65 s which were necessary for all particles to be collected or exhausted in the current simulations (with the “Collected&Trapped” criterion).

The analysis is now done with the other boundary condition for the particle, in which they are collected by touching the bottom wall: It is known from the literature that particles that have entered the hopper may reenter the cyclone (Yoshida et al. (2001); Yoshida (1996)), mostly small-diameter particles. Thus, considering that a particle is collected if it crosses the bottom may not be a realistic condition, and might lead to unrealistic higher grade efficiency. Fig. 6 shows the effect of the two different boundary conditions on the particle grade efficiency. The simulations were performed with the Yakhot turbulence model. The simulation in which particles were only able to leave the cyclone through the overflow (denoted in Fig. 6 as “Escaped”) was interrupted 0.63 seconds after the particles injection. Although the “Escaped” curve matches the experimental better, it is important to highlight that it will change if the simulation continues, as shown above. On the other hand, the “Collected&Trapped” curve is converged.

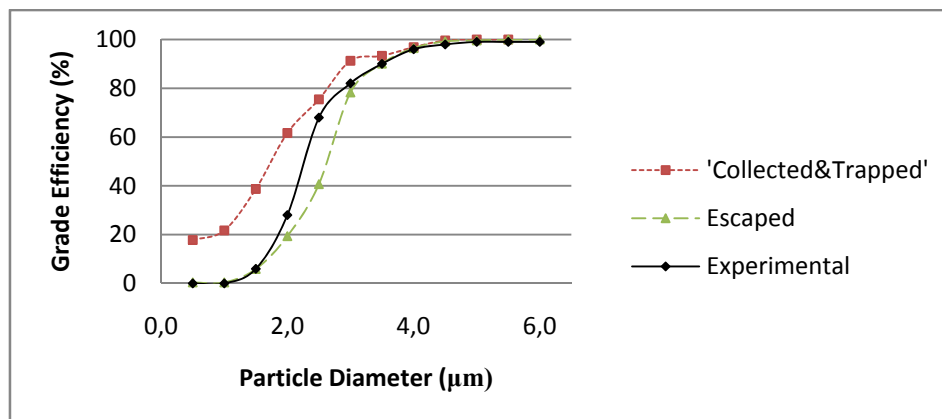


Figure 6. Comparison of particle grade efficiency curves obtained with different boundary conditions for the particulate phase and R. Xiang (2001) experimental data. “Collected & Trapped” is the criterion based on particles that touch the bottom wall, and “Escaped” refers to the collection calculated based on particles injected – escaped.

From Fig. 6, it is possible to see the difference in the cut size diameter (the particle diameter for which the grade efficiency is 50%), which is 2.30 µm in R. Xiang (2001) experiments, nearly 1.71 µm for the “Collected&Trapped” simulations and 2.62 µm for the “Escaped” simulation.

5.3. Effects of turbulence modeling on the separation efficiency

Turbulence modeling is essential in cyclone simulations as it does affect the averaged, instantaneous and RMS velocities fields. In other words, turbulence models will affect the averaged velocity and the turbulent dispersion, and these may be seen as the primary factors for the separation process in a cyclone (Hoffman and Stein, 2008; Derksen, 2003). The separation efficiency based on the second criterion for the three turbulence models is shown in Fig. 7. It is interesting to note that, although the averaged tangential velocity predicted by the DES model is of the same order as the one predicted by the Dynamic turbulence model, which is in turn higher than the tangential velocity predicted by the Yakhot model, its averaged axial velocity field differs considerably from the fields obtained with the other models. In the DES predicted field, the upward velocity in the conical section presents considerably smaller values, and does not present the axial velocity valley in the central region, as shown in Figs. 8 and 9. Besides, the RMS velocities in the DES model are also smaller and concentrated at the cyclone walls, when the RMS velocities for the Dynamic and Yakhot models are higher and concentrated at the cyclone center (which is expected for a cyclone, this shows that the DES model behaved essentially as a RANS model as a result of insufficient grid resolution to activate the LES model). The coupling of these conditions may be translated into a smaller chance for the small particles to reverse their axial movement in the DES simulation. As in the results presented in Fig. 7, the particles that touched the bottom wall were collected (“Collected&Trapped condition), a higher collection efficiency is expected for this model.

The averaged velocity is seen to be higher for the dynamic model. Thus, this may be an explanation for its higher grade efficiency.

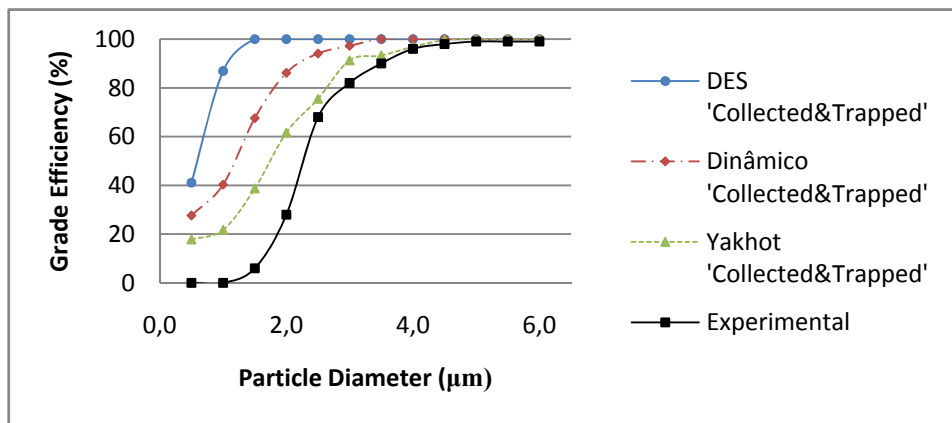


Figure 7. Effect of turbulence modeling on the grade efficiency.

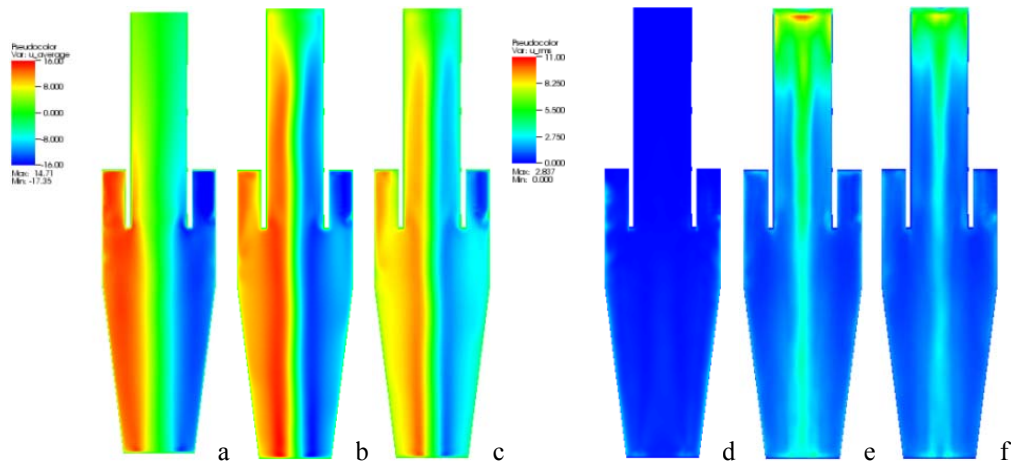


Figure 8. Averaged and RMS tangential velocity fields for the turbulence models. From (a) to (c) averaged tangential velocities, DES, Dynamic and Yakhot turbulence models, respectively. From (d) to (f) RMS tangential velocities, DES, Dynamic and Yakhot turbulence models, respectively.

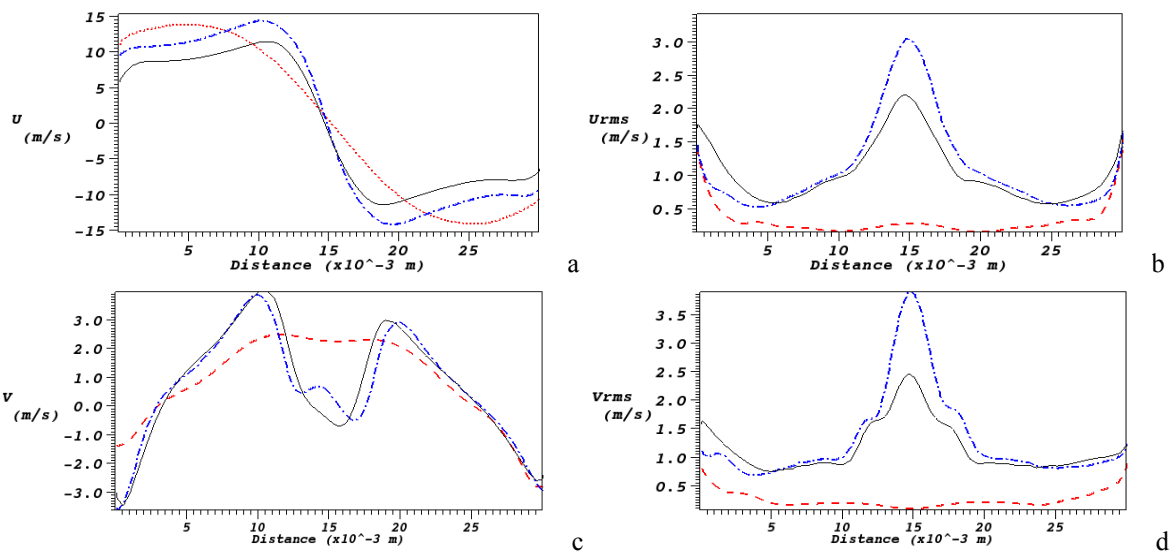


Figure 9. Comparison between averaged and RMS tangential and axial velocity profiles obtained with the three turbulence models in the positions $X=0$ m; $Y=0.05$ m. SST-DES turbulence model; - - - Dynamic turbulence model; — Yakhot turbulence model.

As expected from Figs. 8 and 9, due to their high tangential velocity profiles, the DES and the Dynamic models presented higher pressure drops, 270.85 Pa and 263.74 Pa, respectively. The pressure drop predicted by the Yakhot model was 174.8 Pa, which is good agreement with R. Xiang (2001) experiments, in which the pressure drop was 166 Pa. As these were one-way coupling simulations, the particulate phase does not interfere with the result obtained for the pressure drop.

5.4. Particles paths inside the cyclone

Instantaneous snapshots of particles positions at various different times can be seen in Fig. 10. This data shows aspects normally seen in cyclones, as the dust ring formed in the junction between the cyclone side and top walls, mostly for particles with larger size, Fig. 10-b to Fig. 10-j.

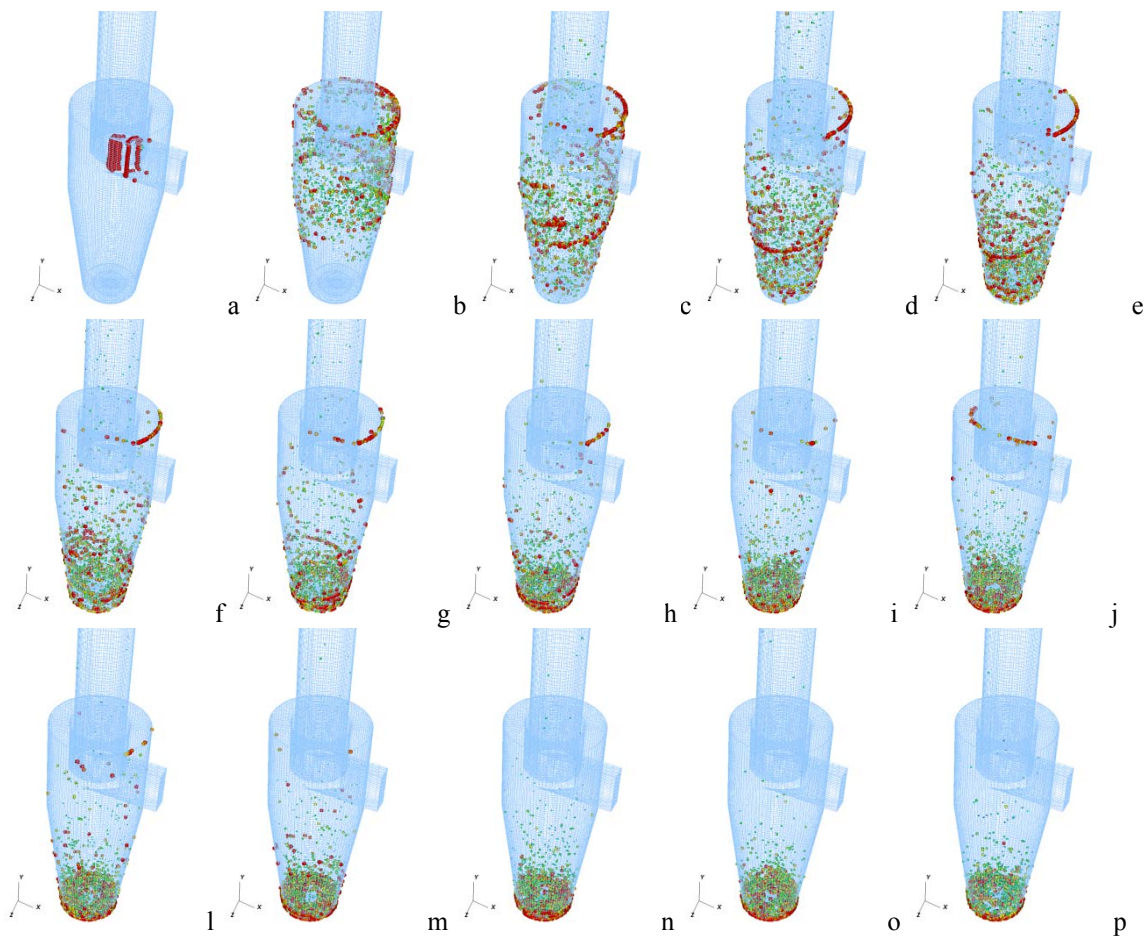


Figure 10. Instantaneous snapshots of the particles position in the simulation whit the Yakhot turbulence model (considering that particles can only leave the cyclone through the overflow – “Escaped” condition). The physical time in each snapshot is: a – 0.01 s; b – 0.1 s; c – 0.2 s; d – 0.3 s; e – 0.4 s; f – 0.5 s; g – 0.6 s; h – 0.7 s; i – 1.0 s; j – 1.07 s; k – 1.5 s; l – 2.0 s; m – 2.5 s; n – 3.0 s; o – 5.0 s; p – 7.5 s.

It is also clear that the solids concentration at the wall form a spiral dust strand, again composed by larger particles, Fig. 10-b to Fig. 10-h.

6. CONCLUSION

A small sampling cyclone operating with a moderate Reynolds number (22,000) was simulated with three different turbulence models, two LES models and one DES model, for the gas phase. The particulate phase was represented by means of a Lagrangian model in an Eulerian framework with one-way coupling between the phases. The influence of turbulence models, turbulent dispersion and boundary conditions for the solid phase were investigated, and the main conclusions are pointed out below:

- The turbulent dispersion is important for particle flow in cyclones;

- The boundary condition for the solid phase is extremely important. Considering that particles that touched the bottom wall were collected (“Collected&Trapped” condition) leads to higher grade efficiency. Considering that particles were only allowed to leave the cyclone through the overflow (“Escaped” condition) leads to an unrealistic, sharp separation curve. These effects would probably be reduced by the use of a hopper, but not fully suppressed. Thus, a better particle-wall collision treatment, may be necessary to model the particulate phase appropriately inside the cyclone.
- The turbulence model used for the gas-phase affect the collection efficiency, but it was found that the RMS velocities have a much larger influence in the collection efficiency than was expected a priori. Attenuated turbulence leads to an increase in the collection efficiency, as reported by other authors. It has to be highlighted that for both the LES and DES simulations, a finer mesh would be necessary for a better prediction of the gas flow field and particulate motion.

7. ACKNOWLEDGEMENTS

The authors would like to thank: FAPEMIG, CAPES and PETROBRAS for the financial support.

8. REFERENCES

- Bernardo, S., “Estudo dos escoamentos gasoso e gás-sólido em ciclones pela aplicação de fluidodinâmica computacional”, 2005, 240 f., Tese de Doutorado, Universidade Estadual de Campinas, São Paulo, Brasil.
- Chuah, T.G., Gimbut, J. and Choong, T.S.Y., 2006, “A CFD study of the effect of cone dimensions on sampling aerocyclones performance and hydrodynamics”, *Power Technology*, Vol. 162, pp. 126-132.
- Derksen, J.J., 2003, “Separation performance predictions of a Stairmand high-efficiency cyclone”, *Fluid Mechanics and Transport Phenomena*, Vol. 49, no 6, pp. 1359-1371.
- Derksen, J.J., Sundaresan, S. and van den Akker, H.E.A., 2006, “Simulation of mass-loading effects in gas-solid cyclone separators”, *Power Technology*, Vol. 163, pp. 59-68.
- Ferziger, J.H. and Peric, M., 2002, “Computational methods for fluid dynamics”, Springer.
- Gronald, G. and Derksen, J.J., 2010, “Simulating turbulent swirling flow in a gas cyclone: a comparison of various modeling approaches”, *Powder Technology*.
- Gujun Wan, Sun. G., Xue, X. and Shi, M., 2008, “Solids concentration simulation of different size particles in a cyclone separator”, *Powder Technology*, Vol. 183, pp. 94-104.
- Haselbacher, A., Najjar, F.M. and Ferry, J.P., 2007, “An efficient and robust particle-localization algorithm for unstructured grids”, *Journal of Computational Physics*, Vol. 225, pp. 2198-2213.
- Hoekstra, A.J., Derksen, J.J. and Van den Akker, H.E.A., “An experimental study of turbulent swirling flow in gas cyclones”, *Chemical Engineering Science*, Vol. 54, pp. 2055-2065.
- Hoffman, A.C., Stein, L.E., 2008, “Gas cyclones and swirl tubes – principles, design and operation”, Second Edition, Springer – Verlag Berlin Heidelberg.
- Lilly, D. K., 1992, “A proposed modification of the Germano subgrid-scale closure method”, *Physics Fluids*, Vol. 4, no 3, pp. 633-635.
- Menter, F.R., 1992, “Improved two equation $k-\omega$ turbulence models for aerodynamic flows”, NASA Technical Memorandum 103975.
- Morsi, S.A. and Alexander, A.J., 1972, “An investigation of particle trajectories in two-phase flow systems”, *J. Fluid Mech.*, Vol. 55, pp. 193-208.
- Narasimha, M., Brennan, M. and Holtham, P.N., 2006, “Large eddy simulation of hydrocyclone – prediction of air-core diameter and shape”, *International Journal of Mineral Processing*, Vol. 80, pp. 1-14.
- Narasimha, M., Brennan, M., Holtham, P.N. and Napier-Nunn, T. J., 2007, “A comprehensive CFD model of dense medium cyclone performance”, *Minerals Engineering*, Vol. 20, pp. 414-426.
- Notay, Y., 2010, “An aggregation-bases algebraic multigrid method”, *Electronic transactions on numerical analysis*, Vol. 37, pp. 123-146.
- Yakhot, A., Orsag, S.A., Yakhot, V. and Israeli, M., 1986, Renormalization group formulation of large-eddy simulation, *J. Scientific Computing*, Vol. 1, pp. 1-51.
- Peltola, J., 2009, “Dynamics in a circulating fluidized bed: experimental and numerical study”, Master of science thesis.
- Pisarev, G.I., Hoffmann, A.C., Peng, W. and Dijkstra, H. A., 2010, “Large eddy simulation of the vortex end in reverse-flow centrifugal separators”, *Appl. Math. Comput.*, DOI: 10.1016/j.amc.2010.07.050
- Shalaby, H.H., “On the potential of large eddy simulation to simulate cyclone separators”, 2007, 1121 f., teses, Von der Fakultät für Maschinenbau der Technischen Universität Chemnitz, Germany.
- Shaohua Li, Hairui Yang, Hai Zhang, Shi Yang, Junfu Lu, Guangxi Yue, 2009, “Measurements of solid concentration and particle velocity distributions near the wall of a cyclone”, *Chemical Engineering Journal*, Vol. 150, pp. 168-173.
- Slack, M.D., Prasad, R.O., Bakker, A. and Boysan, F., 2000, “Advances in cyclone modeling using unstructured grids”, *Institution of Chemical Engineers*, Vol. 78, Part A, pp. 1098-1104.

- Strelets, M., 2001, "Detached eddy simulation of massively separated flows", In 39th AIAA Aerospace Sciences Meeting and Exhibit, American Institute of Aeronautics & Astronautics, Reno, Nv.
- Wegner, B., Maltsev, A., Schneider, C., Sadiki, A., Dreizler, A., and Janicka, J., 2004, "Assessment of unsteady RANS in predicting swirl flow instability based on LES and experiments", *Heat and Fluid Flow*, Vol. 25, pp. 528-536.
- Xiang, R., Park, S.H. and Lee, K.W., 2001, "Effects of cone dimension on cyclone performance", *Journal of Aerosol Science*, Vol. 32, pp. 549-561.
- Yakhot, A., Orsag, S.A., Yakhot, V. and Israeli, M., 1986, Renormalization group formulation of large-eddy simulation, *J. Scientific Computing*, Vol. 1, pp. 1-51.
- Yoshida H., 1996, "Three-dimensional simulation of air cyclone and particle separation by a revised-type cyclone", *Colloids and surfaces*, Vol 109, pp. 1-12.
- Yoshida, H., Fukui, K., Yoshida, K. and Shinoda, E., 2001, "Particle separation by linoya's type gás cyclone", *Powder Technology*, Vol 118, pp. 16-23.

9. RESPONSIBILITY NOTICE

The authors are the only responsible for the printed material included in this paper.